

Symmetry breaking due to Dzyaloshinsky-Moriya interactions in the kagomé lattice

M. Elhajal,* B. Canals,† and C. Lacroix‡

Laboratoire Louis Néel, CNRS, Boîte Postale 166, 38042 Grenoble Cedex 9, France

(Received 5 February 2002; published 10 July 2002)

Due to the particular geometry of the kagomé lattice, it is shown that antisymmetric Dzyaloshinsky-Moriya interactions are allowed and induce magnetic ordering. The symmetry of the obtained low-temperature magnetic phases are studied through mean field approximation and classical Monté Carlo simulations. A phase diagram relating the geometry of the interaction and the ordering temperature has been derived. The order of magnitude of the anisotropies due to Dzyaloshinsky-Moriya interactions are more important than in nonfrustrated magnets, which enhances its appearance in real systems. Application to the jarosites compounds is proposed. In particular, the low-temperature behaviors of the Fe- and Cr-based jarosites are correctly described by this model.

DOI: 10.1103/PhysRevB.66.014422

PACS number(s): 75.10.Jm, 75.30.Ds, 75.50.Ee

I. INTRODUCTION

In the last few years, geometrically frustrated antiferromagnets have been the subject of much experimental and theoretical works.¹ Up to now, the most extensively studied are the kagomé ($D=2$) and the pyrochlore ($D=3$) antiferromagnets. Both are expected to have disordered classical and quantum ground states and behave as spin liquids.^{2,3} In such cases, it is expected that any small perturbation may have a strong effect on the ground-state manifold. These perturbations can arise from thermal or quantum fluctuations, anisotropy, longer range interactions, etc. This paper focuses on the kagomé lattice where it is shown that Dzyaloshinsky-Moriya interactions (DMI's) may be present. As a consequence, magnetic ordering can occur at low temperature. In particular the magnetic structures of the Fe and Cr jarosites⁴⁻⁷ are explored and it is proposed that DMI can explain the low-temperature behaviors of these compounds.

DMI may be present in magnetic systems if there is no inversion center between two magnetic sites. Such interactions between two sites i and j are defined by a vector \mathbf{D}_{ij} : $H_{ij} = \mathbf{D}_{ij}(\mathbf{S}_i \times \mathbf{S}_j)$. It was Moriya⁸ that clarified the conditions for the existence of these interactions and he gave some rules determining the possible directions of \mathbf{D}_{ij} . He proposed a microscopic derivation of these interactions based on Anderson's formalism of superexchange, including spin-orbit coupling. Other mechanisms were proposed for metallic systems with RKKY exchange interactions.^{9,10}

In fact the most general spin hamiltonian for two neighboring spin-1/2 magnetic ions is given by

$$H_{ij} = J_{ij} \mathbf{S}_i \cdot \mathbf{S}_j + \mathbf{D}_{ij}(\mathbf{S}_i \times \mathbf{S}_j) + \mathbf{S}_i \overleftrightarrow{A}_{ij} \mathbf{S}_j, \quad (1)$$

where the second term is the antisymmetric DMI and the last term $\overleftrightarrow{A}_{ij}$ is an anisotropic symmetric exchange interaction. Only antiferromagnetic isotropic exchange ($J_{ij} > 0$) will be considered in the following.

In antiferromagnetic oxides such as α -Fe₂O₃,¹¹ La₂CuO₄,¹² DMI is responsible for weak ferromagnetism. In some Fe and Cr jarosites, a small ferromagnetic component was observed even when the main exchange interaction is antiferromagnetic ($\theta_{CW} \sim -700$ K for Fe jarosites). The

low-temperature magnetic structure is a long-range ordered state where all the spins have the same component in the direction perpendicular to the kagomé plane, giving rise to weak ferromagnetism. The in-plane components of the spins form a $\mathbf{q} = \mathbf{0}$ structure, the three spins of the triangular magnetic unit cell being at 120° one from another. Only one of the two possible chiralities is observed. Depending on the jarosite, the out-of-plane component may vanish.⁴

Each of the magnetic (Fe and Cr) atoms which form the kagomé lattice is surrounded by an octahedron of oxygen atoms, and two neighboring octahedra share one oxygen atom which mediates the superexchange interaction between the magnetic sites. These octahedra are responsible for the crystalline electrical field on the magnetic atoms. They are slightly distorted and their local axial axes are tilted with respect to the normal of the kagomé plane.

In Sec. II, some aspects of DMI specific to the kagomé lattice are discussed and a microscopic derivation of the DMI is made. Sections III and IV deal with the magnetic properties due to the two types of possible DMI. The results are compared to the magnetic structures of the jarosites in Sec. V.

II. DM INTERACTIONS IN THE KAGOMÉ LATTICE

As a consequence of the Hamiltonian being invariant under the symmetry operations which leave the lattice invariant, the direction of \mathbf{D}_{ij} is geometrically constrained and follows rules explicated by Moriya.⁸ In the next section, Moriya's rules are applied to the kagomé lattice and to the related jarosites. In Sec. II B, an estimation of the order of magnitude of the different terms in Eq. (1) is made. Section II C gives a microscopic derivation of DMI following Moriya's formalism and taking into account the peculiar structure and the environment of magnetic atoms in the jarosites.

A. Application of symmetry rules

Two of Moriya's rules give useful informations about the \mathbf{D}_{ij} in the kagomé lattice. First, the middle point between two sites is not a center of inversion for the kagomé lattice, so

DMI are not forbidden by the symmetry of the lattice. Furthermore, in a perfect kagomé lattice, the \mathbf{D}_{ij} can only be perpendicular to the kagomé plane since this plane is a mirror plane. These symmetry considerations determine the axis of all the \mathbf{D}_{ij} vectors (if DMI exist), but not their directions nor their values, which will depend on microscopic details.

In the jarosites, the symmetry is lowered because the octahedra of oxygen atoms which surround the magnetic sites are tilted.^{6,7} The local axial axes of these tetrahedra are not exactly perpendicular to the kagomé plane, and the kagomé plane is then no longer a mirror plane for the lattice when the nonmagnetic atoms are considered. These nonmagnetic oxygen atoms that make up the coordination octahedra must be taken into account because they are responsible for the crystalline electric field on the magnetic atoms, and are involved in the superexchange mechanism between these magnetic sites. Applying Moriya's rules to the jarosites crystal constrains the \mathbf{D}_{ij} vectors to be in the plane perpendicular to the bond (ij) since this is a mirror plane of the jarosite structure.

In both the pure kagomé and jarosite structures, the \mathbf{D}_{ij} are not completely determined by symmetry. However, if we fix arbitrarily one of the \mathbf{D}_{ij} , then all the others are fixed by the threefold rotation axis perpendicular to the kagomé plane that passes through the center of the triangles of the kagomé lattice.

Moriya's rules constraint the \mathbf{D}_{ij} vectors with the help of the symmetry of the lattice, but they are not a proof of the existence of DMI in the kagomé lattice (or the related jarosites), they just express the fact that *if* DMI are present, then the \mathbf{D}_{ij} will necessarily be restricted to some set of possible vectors.

B. General considerations

Taking into account the superexchange mechanism, the isotropic exchange J_{ij} is proportional to t_{ij}^2/U (t_{ij} being the intersite hopping and U the on-site Coulomb repulsion), while it was shown by Moriya that $|\mathbf{D}_{ij}|$ is proportional to $\lambda t_{ij}^2/\Delta U$ (λ being the spin-orbit coupling and Δ the crystal field splitting) and \vec{A}_{ij} is proportional to $\lambda^2 t_{ij}^2/\Delta^2 U$. This last term, being one order of magnitude smaller than the DMI is often neglected. However, it was suggested by Shekhtman *et al.*¹³ that it plays an important role, as does the DMI, because they are responsible for anisotropies respectively proportional to D^2/J and A which are of the same order of magnitude. This argument is based on the assumption that the isotropic exchange J , which is the dominant interaction favors collinear configurations, and is untrue in the case of the kagomé lattice due to its frustration. In a collinear structure DMI are in competition with isotropic exchange J resulting in D^2/J anisotropy, whereas anisotropic symmetrical exchange defines easy axes or planes but is not contradictory with a collinear structure, resulting in $\sim A$ anisotropy. Considering different possible \vec{A}_{ij} , we find that these arguments generally do not hold in the case of a noncollinear structure such as those found on the kagomé lattice. Rather, the anisotropies are respectively of the order of D and A , which is the reason why only DMI will be taken into account in this

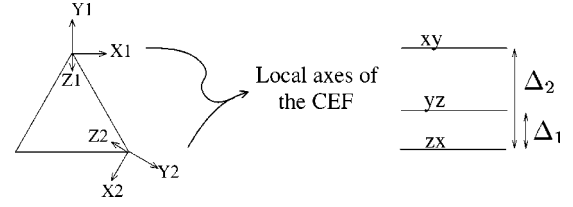


FIG. 1. Local axes of the crystalline electrical field considered in the microscopic derivation of the DMI. The axes are tilted by an angle α around the x axis toward the center of the triangle.

work. The anisotropic exchange \vec{A} is considered to enter the problem at the next order of perturbation theory.

Shekhtman *et al.* also showed that under specific symmetry conditions it was possible to map the total spin Hamiltonian of Eq. (1) onto an isotropic Heisenberg Hamiltonian [only the first term of Eq. (1)] thus recovering a hidden rotational symmetry. In fact, such a “local gauge transformation” was previously considered by Kaplan¹⁴ for the one-dimensional Hubbard model with spin-orbit coupling. It is always possible to make this “local” transformation involving two spins, but since one spin interacts with several neighbors, the symmetry of the lattice must allow for a “global” transformation in order to recover a hidden rotational symmetry (see Ref. 13 for more details). On the kagomé lattice, this mapping to an isotropic Heisenberg Hamiltonian is not possible and no rotational symmetry is recovered.

C. Microscopic derivation of DMI using Moriya's technique

As mentioned above, while application of Moriya's rules restricts the \mathbf{D} to some set of possible vectors, they are not proof of the existence of DMI. In this section we derive DMI using the method proposed by Moriya assuming some microscopic situation (orbitals and crystalline electric field) which is arbitrary, but related to the case of the jarosites. The method proposed by Moriya applies for localized magnetic electrons (insulators). In order for the derivation to be manageable, we assume that the ground state is not degenerate due to crystal electrical field (except Kramers spin degeneracy) and each magnetic site is occupied by one electron. In our case, we consider the t_{2g} orbitals, whose degeneracy has been further lifted by some distortion of the octahedral environment. The e_g orbitals are assumed to be at a much higher-energy level (or completely filled and at much lower-energy level). The crystalline field scheme for the t_{2g} is represented on Fig. 1. The three states of each triangle are obtained from one another by a rotation of $2\pi/3$ around the axis perpendicular to the kagomé plane.

The octahedral symmetry and the $3d$ orbitals are relevant for the jarosites (see Sec. I), and the lifting of degeneracy of the t_{2g} orbitals is supported by the fact that the oxygen octahedra surrounding magnetic sites are distorted in the jarosites (see Figs. 2 and 3 of Ref. 15). The local axes of the crystalline field on each site have also been tilted towards the center of the triangles of the kagomé lattice by an angle α , in order to fit with the jarosites symmetry. Spin-orbit coupling is taken into account at first order in perturbation theory as it is expected to be much smaller than the crystalline electric

field. Next, the on-site Coulomb repulsion is assumed to be much higher than the hopping term, and the intersite hopping is introduced to second order in perturbation. Doing so, we arrive at the following expression for the \mathbf{D}_{12} vector

$$D_x = \sqrt{3}D_y, \quad (2)$$

$$D_y = \frac{\lambda\sqrt{3}}{256U} \sin(2\alpha) f_1(\alpha) \left(\frac{f_2(\alpha)}{\Delta_1} + \frac{9}{\Delta_2} [(dd\delta) - (dd\sigma)] \right), \quad (3)$$

$$D_z = -\frac{\lambda\sqrt{3}\cos^2\alpha}{32U\Delta_1} f_1(\alpha) f_2(\alpha), \quad (4)$$

where

$$f_1(\alpha) = 4(dd\pi) - 9(dd\sigma)\sin^2\alpha - 3(dd\delta)(1 + 3\cos^2\alpha), \quad (5)$$

$$f_2(\alpha) = 4(dd\pi)(3\cos^2\alpha - 2) - 9(dd\sigma)\sin^2\alpha + (dd\delta)(1 + 3\cos^2\alpha). \quad (6)$$

$(dd\sigma)$, $(dd\pi)$, and $(dd\delta)$ are the transfer integrals as defined by Slater and Koster.¹⁶

The obtained \mathbf{D}_{ij} vectors are located in the plane perpendicular to the (ij) bond and are perpendicular to the kagomé plane if the octahedra are not tilted ($\alpha=0$) as they should according to Moriya's rules.

III. CASE OF $\mathbf{D} \perp$ KAGOMÉ PLANE

In this section the consequences of the DMI on the low-temperature magnetic structure are explored in the case where \mathbf{D} is perpendicular to the kagomé plane. Both cases $D_z > 0$ and $D_z < 0$ (z is the axis perpendicular to the kagomé plane and the convention is taken that the spins in the cross products appear rotating anticlockwise around the hexagons) are considered through mean field approximation and Monte Carlo simulations with classical Heisenberg spins.

Looking for $\mathbf{q}=\mathbf{0}$ structures, a restriction which will be justified by Monte Carlo simulations, it is found that within mean field approximation, the system undergoes a phase transition to a long range ordered state. In the ordered state, all the spins lie in the kagomé plane, so one effect of the DMI is to act as an easy-plane anisotropy (as long as the first excitations are not taken into account, e.g., looking only at the structure of the ground state). As it can be easily seen by expanding the cross product with only a z component for the \mathbf{D}_{ij} , the Hamiltonian is invariant under a global rotation of all the spins around the z axis. This degree of freedom is of course still present for the ground state. Since it is a $\mathbf{q}=\mathbf{0}$ structure, all triangles have the same magnetic structure. Depending on the sign of D_z , two chiralities are found and represented on Fig. 2.

In order to study the behavior of this system at finite temperatures, Monte Carlo simulations have been performed on finite size clusters with classical Heisenberg spins. In particular, the behavior of the critical temperature as a function of D/J is plotted in Fig. 3. The critical temperature was

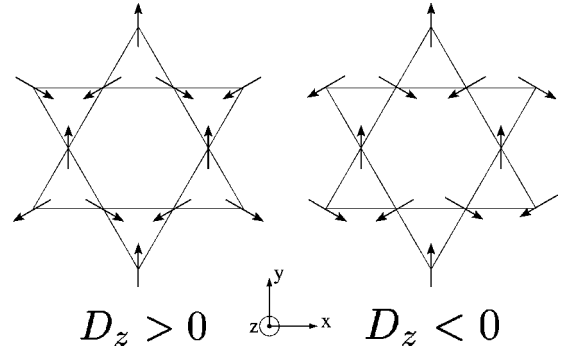


FIG. 2. $D \perp$ kagomé plane. The spins lie in the kagomé plane and the sign of D_z selects the chirality. There is a global rotational degree of freedom around the z axis.

taken as the maximum of the specific heat.

The line $D=0$ on Fig. 3 represents the well studied (classical) kagomé lattice with antiferromagnetic nearest-neighbor exchange interactions. This system shows partial order: the coplanar states are asymptotically selected as temperature is lowered² (order by disorder). However, as soon as D has a finite value, even much smaller than J , a phase transition occurs at *finite* temperature. For this reason the low-temperature magnetic structure will be governed by DMI. It must be emphasized that this argument holds because DMI selects a peculiar set of magnetic states, and does not have a complete branch of zero modes excitations as it is the case for the exchange for the sole isotropic Heisenberg model. This is supported by the fact that the critical temperature is almost linear in D , and only weakly dependent on the strength of the antiferromagnetic exchange interactions (J). The physical reason for this is also that the long-range ordered states which are imposed by DMI are part of the degenerate ground states of the system with only isotropic exchange (J) interactions, even after a partial lifting of degeneracy due to thermal fluctuations. Thus, DMI has here a first order effect on a degenerate ground state, while usually DMI acts as a small perturbation on antiferromagnetically ordered ground state, leading to second order corrections.

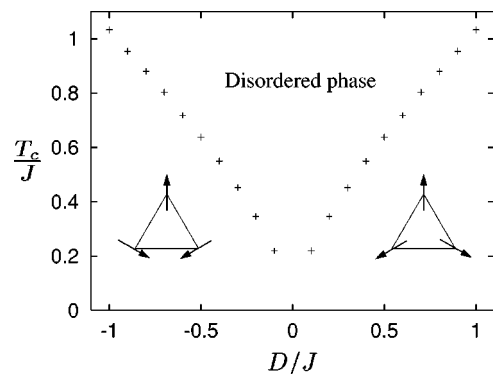


FIG. 3. Critical temperature as a function of D/J in the case of $D \perp$ kagomé plane. The critical temperature is $\sim D$. The coplanar $\mathbf{q}=\mathbf{0}$ low-temperature magnetic structures are represented.

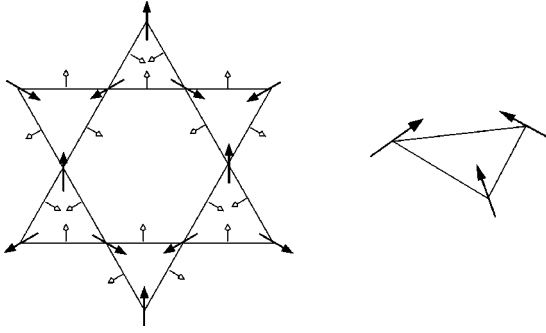


FIG. 4. In-plane \mathbf{D} represented in the middle point between the magnetic sites and the associated magnetic structure. All the spins have a weak z component resulting in weak ferromagnetism. There is no global rotational degeneracy.

IV. CASE OF TILTED OXYGEN TETRAHEDRA

In this section we study the general case where \mathbf{D}_{ij} is in the plane perpendicular to the (ij) bond. In order to clarify the discussion, we start by looking at the sole effect of the in-plane component of \mathbf{D} before turning to the general case.

A. Case of \mathbf{D} in the kagomé plane : canted structure

The \mathbf{D} vectors as well as the ground state magnetic configuration obtained by mean field approximation and Monte Carlo simulations are represented on Fig. 4.

The structure has some similarities with the $D_z > 0$ case for $\mathbf{D} \perp$ kagomé plane, and indeed it has the same chirality, but there are also big differences. The spins do not lie in the kagomé plane anymore, but they all have the same out-of-plane z component, giving rise to weak ferromagnetism, perpendicular to the kagomé plane. Changing the sign of the in-plane component of \mathbf{D} changes the sign of the z component of the spins as can be easily seen by expanding the cross product in the Hamiltonian. A second difference is that there is no longer a global rotational degree of freedom and each spin points towards a fixed direction. In this case, DMI seems to act more similar to an easy-axis anisotropy. The ground state for the DMI alone does not belong to the ground state manifold for the exchange interactions, since the sum of the spins on each triangle is not zero and there is now a competition between exchange and DMI. The consequence of this competition is that the angle between the spins and the kagomé plane depends now on D/J : this angle, as well as the weak ferromagnetic component, increases with D/J .

B. General case

We now turn to the general case where \mathbf{D}_{ij} lies in the plane perpendicular to the (ij) bond. If $D_z > 0$ then the chirality which is selected by D_z is the same as the one which comes from the in-plane component D_p . Starting from the configuration for $D_z = 0$, the effect of D_z on the lowest-energy configuration will be very much the same as J : it will decrease the value of the angle between the spins and the kagomé plane. The case $D_z < 0$ is more complicated: the chirality favored by D_z is not the same as the one which is selected if only the in-plane component of D is considered.

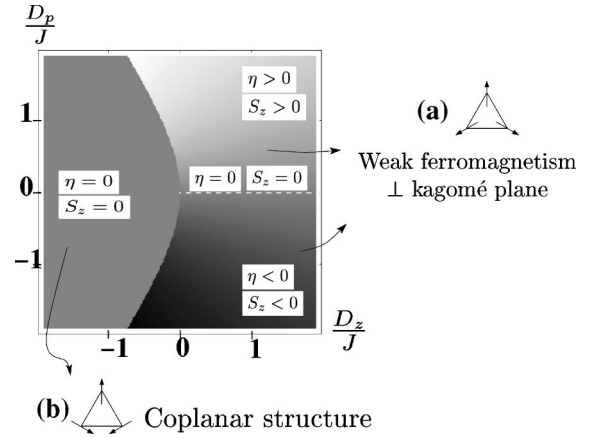


FIG. 5. Ground states obtained for different values of J (isotropic exchange), D_p and D_z (in plane and out of plane components of \mathbf{D}). The intensity of the gray represents η , the angle between the spins and the kagomé plane. $\eta = 0$ corresponds to a structure where the spins lie in the kagomé plane with zero out of plane component $S_z = 0$ (this is represented by the homogeneous grey color on the left part as well as the dashed line on the right part). For the weak ferromagnetic structures with an out of plane magnetic component $S_z \neq 0$, the intensity of white (black) is proportional to the positive (negative) value of η .

The result is a competition between the in-plane and the out-of-plane components of \mathbf{D} . When \mathbf{D} is almost in the kagomé plane with a small negative component along the z axis, then the canted structure is selected with a ferromagnetic moment which increases with increase of the z component. There is a critical value of D_z/D_p , and if D_z is negative enough, then the ground state is no longer the canted structure, but the planar structure on the right of Fig. 2, as in the case of $\mathbf{D} \perp$ kagomé plane. This critical value depends on the strength of the exchange interactions J , since the latter favor the planar structure.

It appears that the magnetic structures for \mathbf{D} and $-\mathbf{D}$ are not always similar as in the case of $\mathbf{D} \perp$ to the kagomé plane. They can not be deduced easily from each other. This can also be seen on the Hamiltonian: when replacing \mathbf{D} by $-\mathbf{D}$, there is no simple transformation of the \mathbf{S}_i which would leave the Hamiltonian invariant. This comes from the fact that the lattice is not bipartite, since in a bipartite lattice, exchanging the two sublattices would transform $\mathbf{S}_i \times \mathbf{S}_j$ into $-\mathbf{S}_i \times \mathbf{S}_j$ and leave the Hamiltonian invariant. However, $D_p \rightarrow -D_p$ corresponds to a trivial symmetry: changing simultaneously $S_z \rightarrow -S_z$ will leave the Hamiltonian invariant, and so the nontrivial part of the transformation $\mathbf{D} \rightarrow -\mathbf{D}$ comes from the z component D_z . The discrepancy between the structures for \mathbf{D} and $-\mathbf{D}$ is illustrated on Fig. 5. It represents the different ground states obtained for different values of the parameters D_p , D_z , and J .

This figure was obtained by comparing the energies of the two possible chiralities (a) and (b) (see Fig. 5) on one triangle, and minimizing with respect to η , the angle between the spins and the kagomé plane and the angle φ between the projection of the spins on the kagomé plane and their position as represented on Fig. 5. The energies of the two triangles (a) and (b) are

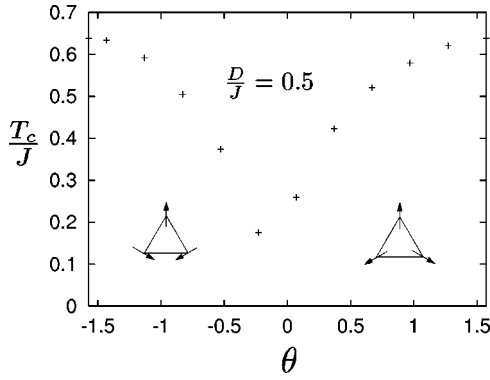


FIG. 6. Critical temperature as a function of the angle θ between \mathbf{D} and the kagomé plane, for a fixed value of $D = \sqrt{D_p^2 + D_z^2}$.

$$\frac{E_a}{N} = \frac{J}{2} [1 - 3 \cos(2\eta)] - \sqrt{3} D_z \cos^2 \eta - \sqrt{3} D_p \sin(2\eta) \cos \varphi, \quad (7)$$

$$\frac{E_b}{N} = \frac{J}{2} [1 - 3 \cos(2\eta)] + \sqrt{3} D_z \cos^2 \eta. \quad (8)$$

Several aspects already mentioned appear in these expressions. First, the sign of D_z selects the chirality since it appears with a different sign in E_a and E_b . D_p appears to favor chirality (a) and weak ferromagnetism perpendicular to the kagomé plane ($\eta \neq 0$). For chirality (a), if $D_p = 0$, the spins lie in the kagomé plane ($\eta = 0$), and there is a global rotational degree of freedom since the energy would not depend on φ . If chirality (b) is selected, then $\eta = 0$ always minimizes the energy (even for $D_p \neq 0$) and so only in-plane structures appear with this chirality and the global rotational degree of freedom is always present. Furthermore, in this case the energy does not depend on D_p .

When chirality (a) is selected, and $D_p \neq 0$, the spins have an out of plane component with the angle between the spins and the kagomé plane being

$$\tan(2\eta) = \frac{2D_p}{\sqrt{3}J + D_z}. \quad (9)$$

In this case, $\varphi = 0$ (no global rotational degree of freedom).

Figure 6 shows the evolution of the critical temperature as a function of the angle θ between \mathbf{D} and the kagomé plane.

The critical temperature is lower when \mathbf{D} is in the kagomé plane ($\theta = 0$) than when \mathbf{D} is perpendicular ($\theta = \pm \pi/2$). This is easily understood since for \mathbf{D} in the kagomé plane, DMI favors a canted structure, which is not a lowest energy configuration for the isotropic exchange part of the Hamiltonian (J). For $\theta = \pm \pi/2$, DMI selects a coplanar structure, which also minimizes the isotropic exchange.

The fact that the critical temperature is not symmetrical with respect to $\theta = 0$ (Fig. 6) also illustrates the different behavior for \mathbf{D} and $-\mathbf{D}$. Indeed, changing $\theta \rightarrow -\theta$ corresponds to $D_z \rightarrow -D_z$ which is the nontrivial part of the transformation $\mathbf{D} \rightarrow -\mathbf{D}$, because $D_p \rightarrow -D_p$ corresponds to the trivial symmetry $S_z \rightarrow -S_z$. The fact that the critical temperature is always different for symmetrical values of θ with

respect to 0 is due to the fact that $D_z < 0$ is in competition with the in-plane component of \mathbf{D} since they tend to select different chiralities; on the contrary $D_z > 0$ and D_p drive the system to the same chirality, hence a higher critical temperature is obtained for $\theta > 0$ than for $\theta < 0$.

V. MAGNETIC STRUCTURE OF FE AND CR JAROSITES

We are interested here in the low-temperature magnetic structure of the Fe- and Cr-based jarosites, where the magnetic ions (Fe^{3+} and Cr^{3+}) form kagomé planes which are stacked one on another^{4-7,15} giving rise to a three-dimensional structure. However, the magnetic behavior of the jarosites is believed to be essentially that of a (two-dimensional) kagomé lattice, because the different kagomé planes are fairly well separated by several nonmagnetic atoms implying that the superexchange interactions between neighboring planes are much weaker than between magnetic sites belonging to the same kagomé plane. These magnetic sites are surrounded by octahedra of oxygen atoms responsible for the crystalline electrical field and involved in the superexchange interactions. These octahedra are slightly distorted and tilted (see Figs. 2 and 3 of Ref. 15) which is consistent with the microscopic electronic states we have considered for our microscopic derivation of DMI.

A long-range ordered state is observed experimentally in these compounds,^{4-7,15} and the low-temperature magnetic structure has an ordering wave vector $\mathbf{k} = (0,0,0)$ or $\mathbf{k} = (0,0,\frac{3}{2})$, depending on the diamagnetic atoms present in the compound. The third component of the \mathbf{k} vector corresponds to the propagation of the magnetic structure from one kagomé plane to another and is due to weak interplane superexchange interactions which were not considered in this article since they play no role in the ordering of one kagomé plane.

Henceforth the ordering of only one kagomé plane is considered. The different observed magnetic structures have a $\mathbf{q} = \mathbf{0}$ wave vector and always correspond to chirality (a). Both planar and weak-ferromagnetic (all the spins having the same z component along the axis perpendicular to the kagomé plane) structures are observed experimentally and both are obtained here theoretically. The planar structure with chirality (b) obtained theoretically is not observed experimentally in these jarosites.

The experimental structures can also be obtained introducing a single-ion anisotropy,^{5,7} however, this is not a relevant interaction at least in the case of Fe jarosites. Indeed, the magnetic ions are Fe^{3+} , and so the $3d$ orbitals are half filled, with five electrons coupled giving rise to a spin $S = \frac{5}{2}$. Thus, the charge distribution is spherical for this orbital occupancy, and consequently prevents the appearance of a spin anisotropy. Also for Cr^{3+} ions, the 3 t_{2g} orbitals are filled ($S = \frac{3}{2}$) and the single ion anisotropy should be small.

VI. CONCLUSIONS

It has been shown that DMI are allowed by the symmetry of the kagomé lattice and are relevant interactions whose

effect is enhanced by the frustration of the predominant antiferromagnetic isotropic exchange. A microscopic derivation of these interactions for a schematic electronic configuration somewhat related to the jarosites structure was done. The magnetic properties due to DMI were studied through mean field approximation and Monte Carlo simulations. Contrarily to the predominant antiferromagnetic isotropic exchange, DMI can induce several long range ordered magnetic structures depending on the different microscopic parameters J ,

D_p , and D_z . The low-temperature magnetic structures of the Fe- and Cr-based jarosites can be explained by the presence of DMI. This is an example of a compound where magnetic ordering is not due to exchange interactions but to DMI.

ACKNOWLEDGMENT

It is a pleasure to acknowledge Dr. Andrew Wills for fruitful discussions.

*Electronic address: elhajal@grenoble.cnrs.fr

†Electronic address: canals@grenoble.cnrs.fr

‡Electronic address: lacroix@grenoble.cnrs.fr

¹For a collection of articles, see *Magnetic Systems with Competing Interactions: Frustrated Spin System*, edited by H. T. Diep (World Scientific, Singapore, 1994); for Ising systems, see R. Liebmann, *Statistical Mechanics of Periodic Frustrated Ising Systems* (Springer, Berlin, 1986); for reviews, see A. P. Ramirez, *Annu. Rev. Mater. Sci.* **24**, 453 (1994); P. Schiffer and A. P. Ramirez, *Comments Condens. Matter Phys.* **18**, 21 (1996); M. J. Harris and M. P. Zinkin, *Mod. Phys. Lett. B* **10**, 417 (1996).

²J.T. Chalker, P.C.W. Holdsworth, and E.F. Shender, *Phys. Rev. Lett.* **68**, 855 (1992).

³P. Lecheminant, B. Bernu, C. Lhuillier, L. Pierre, and P. Sindzinger, *Phys. Rev. B* **56**, 2521 (1997).

⁴A.S. Wills, *Phys. Rev. B* **63**, 064430 (2001).

⁵T. Inami, T. Morimoto, M. Nishiyama, S. Maegawa, Y. Oka, and

H. Okumura, *Phys. Rev. B* **64**, 054421 (2001).

⁶A.S. Wills, A. Harrison, C. Ritter, and R.I. Smith, *Phys. Rev. B* **61**, 6156 (2000).

⁷T. Inami, M. Nishiyama, S. Maegawa, and Y. Oka, *Phys. Rev. B* **61**, 12 181 (2000).

⁸T. Moriya, *Phys. Rev.* **120**, 91 (1960).

⁹D.A. Smith, *J. Magn. Magn. Mater.* **1**, 214 (1976).

¹⁰A. Fert and P.M. Levy, *Phys. Rev. Lett.* **44**, 1538 (1980).

¹¹I. Dzyaloshinsky, *Sov. Phys. JETP* **5**, 1259 (1957).

¹²D. Coffey, T.M. Rice, F.C. Zhang, *Phys. Rev. B* **44**, 10 112 (1991).

¹³L. Shekhtman, O. Entin-Wohlman, and A. Aharony, *Phys. Rev. Lett.* **69**, 836 (1992).

¹⁴T.A. Kaplan, *Z. Phys. B: Condens. Matter* **49**, 313 (1983).

¹⁵A.S. Wills, *Can. J. Phys.* **11-12**, 1501 (2001).

¹⁶J.C. Slater and G.F. Koster, *Phys. Rev.* **94**, 1498 (1954).